ACS Catalysis

Research Article

Cite This: ACS Catal. 2018, 8, 8796−8803

pubs.acs.org/acscatalysis

Decoupling Catalysis and Chain-Growth Functions of Mono(μ-alkoxo)bis(alkylaluminums) in Epoxide Polymerization: Emergence of the N−Al Adduct Catalyst

Jennifer Imbrogno,[†,§] Robert C. Ferrier, Jr.,[†,∥] Bill K. Wheatle,[†] Michael J. Rose,[‡] and Nathaniel A. Lynd*[,†,§]

[†]McKetta Department of Chemical Engineering, [‡]Department of Chemistry, and [§]Center for Dynamics and Control of Materials, The University of Texas at Austin, Austin, Texas 78712, United States

Supporting Information

ABSTRACT: A mono(μ-oxo)bis(alkylaluminum) (MOB) catalyst and initiator for epoxide polymerization, $[(H_3C)_2NCH_2CH_2(\mu_2\text{-}O)Al(iBu)_2{\cdot}Al(iBu)_3]$ (**1**), produced a ca. 170-fold enhancement in epoxide polymerization rate over previously reported MOB initiators demonstrated with allyl glycidyl ether (AGE). This discovery reduces polymerization times to minutes. **1** exhibited an exponential dependence of polymerization rate on concentration, rather than an expected low integer order relationship. A proposed polymerization intermediate was identified via direct synthesis, isolation, kinetic comparison, and corroborating in situ spectroscopic evidence to be a symmetric bis((μ-alkoxo)-dialkylaluminum) (BOD) with a characteristic $R_3N{\cdot}AlR'_3$ (N−Al) adduct. The N−Al adduct on the BOD intermediate is proposed to act as a catalyst, whereas the aluminoxane ring is proposed to be the site of monomer enchainment on the basis of mass spectrometry and spectroscopic analysis of resultant polymer structure. The distinct catalytic and initiation/propagation functionalities were separated into separate species, and the catalytic activity of the N−Al adduct was demonstrated in the presence of a distinct aluminoxane initiator. Each 1 equiv of N−Al adduct relative to initiator resulted in an abrupt (ca. 5−10-fold) increase in the polymerization rate of AGE. The resultant N−Al adduct catalyst represents a versatile tool for rapid functional macromolecular synthesis.

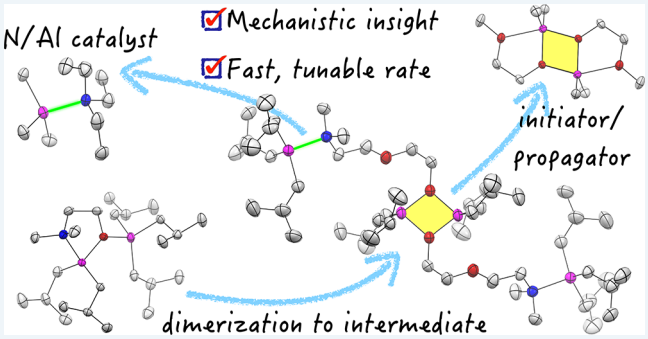

KEYWORDS: *aluminum, Lewis pair, N−Al adduct, polyether, polymerization catalysis*

INTRODUCTION

Epoxide-based polyethers enable compositional control of structure−property relationships in a macromolecular platform due to the wide variety of available monomers and the relatively indiscriminate ring-strain driving force for polymerization.[1,2] In spite of the versatility offered by epoxides as monomers, no general-use, consensus technique for epoxide polymerization for nonspecialists has emerged in common usage in the same sense that it has for many other monomer classes such as vinyls,[3] cyclic olefins,[4,5] and lactones.[6−9] While anionic ring-opening polymerization (AROP) has served as the de facto consensus polymerization technique for epoxides, only lower molecular weights are generally obtainable for any epoxide except for the simplest case, ethylene oxide.[10−12] The performance of AROP is sensitive to, and varies widely with, monomer structure,[13] and chain transfer to monomer limits control of the chain-end functionality and control of molecular weight in many systems.[12]

Numerous catalytic strategies for epoxide polymerization have been reported to provide access to high[14] and controlled molecular weight materials possessing narrow dispersities[15−17] and controlled stereochemistry.[14,18−23] These valuable contributions have expanded the mechanistic understanding of epoxide polymerization and provided synthetic access to novel materials. Our work focuses on establishing a polymerization method that is easy to use, is based on Earth-abundant metals such as aluminum,[24−28] is characteristically "living",[29−34] and provides control of chain-end functionality[35,36] and functional group tolerance.[37]

Recently reported mono(μ-alkoxo)bis(alkylaluminum) (MOB) compounds combine many of the advantages of the catalytic approaches (i.e., tolerance of monomer functionality) and exhibit a degree of control to epoxide polymerizations consistent with living controlled polymerization with neither autotermination nor chain transfer with associated control of molecular weight via the polymerization stoichiometry. The MOB initiators are trivial to synthesize and use and under controlled conditions provide stoichiometric control over

Received: June 24, 2018
Revised: August 2, 2018
Published: August 9, 2018

DOI: 10.1021/acscatal.8b02446
ACS Catal. 2018, 8, 8796−8803

molecular weight, end-group structure, versatility in monomer substrates, and macromolecular architecture.[37,38] Scheme 1 shows the molecular structure of the MOB initiator (**1**) utilized in this work and general polymerization scheme.

Scheme 1. Effectiveness of Mono(μ-oxo)bis(alkylaluminum) (MOB) $[(Me)_2NCH_2CH_2(\mu_2\text{-}O)Al(iBu)_2{\cdot}Al(iBu)_3]$ (1) Initiators for General and Rapid Epoxide Polymerization

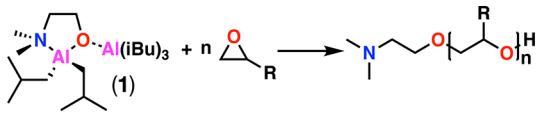

In the original report of MOB initiator synthesis and activity for polymerization, $[(Bn)_2NCH_2CH_2(\mu_2\text{-}O)Al(Et)_2{\cdot}Al(Et)_3]$ (**2**) required days for complete consumption of monomer.[38] We later investigated the effect of simple alkylaluminum substitution, which led to a 4-fold increase in polymerization rate.[37] In this report, we observed an unexpected and substantial increase in polymerization rate of ca. 100-fold over our originally reported MOB initiator via a change in alkylamine substitution. The polymerization rate was found to depend unusually strongly on MOB (**1**) concentration. These results were obtained with $[(Me)_2NCH_2CH_2(\mu_2\text{-}O)Al(iBu)_2{\cdot}Al(iBu)_3]$ (**1**) shown in Scheme 1 and Figure 1, which required only minutes for complete consumption of allyl glycidyl ether (AGE) to 10000 g/mol of poly(allyl glycidyl ether) (PAGE). The dramatic increase in rate associated with a relatively simple structural change of the initiator prompted us to further explore the mechanistic aspects of MOB-initiated polymerizations with isolation of a potential polymerization intermediate that was substantiated upon further investigation. The intermediate was characterized as the product of MOB dimerization with migration of the datively bound trialkylaluminum to the amine. This transformation yielded a symmetric bis((μ-alkoxo)dialkylaluminum) (BOD) with the aluminum alkoxide serving as the site of monomer enchainment and the $R_3N{\cdot}AlR'_3$ moiety serving as catalyst. The enchainment and catalytic functionalities were ultimately decoupled into distinct chemical entities, creating a new, two-component, versatile platform for functional epoxide polymerization.

RESULTS AND DISCUSSION

Remarkable Polymerization Rate Increase with $[(H_3C)_2NCH_2CH_2(\mu_2\text{-}O)Al(iBu)_2{\cdot}Al(iBu)_3]$ (1) Relative to Homologous Mono(μ-alkoxo)bis(alkylaluminum) Species 2–4. A new MOB initiator was synthesized from (dimethylamino)ethanol and triisobutylaluminum, resulting in **1**, which was crystallized directly from the reaction medium and characterized by X-ray crystallography (structure shown in Figure 1a) and NMR spectroscopy as shown in Figures S1 and S9 and Tables S1–S6 in the Supporting Information. Previously published MOB structures as synthesized from (dibenzylamino)ethanol and triethyl (**2**)-, trimethyl (**3**)-, and triisobutylaluminum (**4**) are also shown in Figure 1a.[37,38] As with other MOB structures, the new $[(Me)_2NCH_2CH_2(\mu_2\text{-}O)Al(iBu)_2{\cdot}Al(iBu)_3]$ (**1**) exhibited strong structure–kinetics relationships for epoxide polymerization.

Neat polymerizations were conducted to compare the rates among new (**1**) and previously reported homologous MOB initiators (**2**–**4**). The monomer to initiator ratio was selected to create a 10000 g/mol of poly(allyl glycidyl ether) (PAGE) at 100% conversion of allyl glycidyl ether (AGE): $[AGE]_0/[MOB]_0 = 87$. The polymerization using **1** was complete after

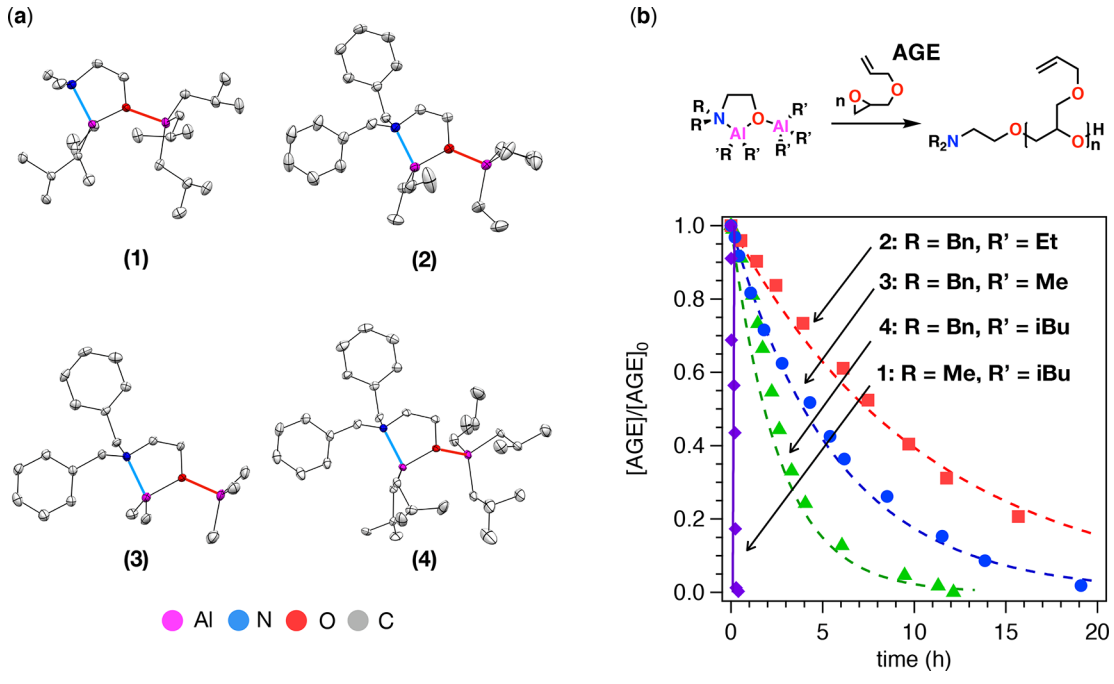

Figure 1. (a) Structures of $[(H_3C)_2NCH_2CH_2(\mu_2\text{-}O)Al(iBu)_2{\cdot}Al(iBu)_3]$ (**1**), $[(Bn)_2NCH_2CH_2(\mu_2\text{-}O)Al(Et)_2{\cdot}Al(Et)_3]$ (**2**),[36] $[(Bn)_2NCH_2CH_2(\mu_2\text{-}O)Al(Me)_2{\cdot}Al(Me)_3]$ (**3**),[35] and $[(Bn)_2NCH_2CH_2(\mu_2\text{-}O)Al(iBu)_2{\cdot}Al(iBu)_3]$ (**4**).[35] All ellipsoids are shown at 50% probability, and Bn = benzyl. (b) Incremental increase in the rate of epoxide polymerization initiated with MOB complexes from **2** to **4** as alkyl substitution on aluminum was changed. **1** represents a disproportionate increase in polymerization rate with a change in alkyl substitution on nitrogen. **1** concludes a polymerization of allyl glycidyl ether (AGE) in minutes.

DOI: 10.1021/acscatal.8b02446
ACS Catal. 2018, 8, 8796–8803

ca. 20 min and produced a large exotherm presumably from the rapid release of epoxide ring strain energy (ca. 25 kcal/mol),[39] raising the unbuffered reaction temperature of the polymerization to ca. 80 °C as measured by the in situ ReactIR 15 FTIR probe. The conversion of AGE, as determined by ^{1}H NMR spectroscopy of the crude reaction mixture, was quantitative, and the number-average molecular weight (M_n), determined by size exclusion chromatography (SEC) with refractive index, viscometer, and light scattering detection, was 9400 g/mol with a molecular weight dispersity ($Đ$) of 1.15. To quantitatively compare rates of polymerization, we report apparent rate constants (k_{app} in s^{-1}) by fitting the time-dependent consumption of monomer to $[AGE]/[AGE]_0 = e^{-k_{app}t}$ or $-\ln[AGE]/[AGE]_0 = k_{app}t$. The apparent rate constants (k_{app} in s^{-1}) are compared for neat polymerizations of AGE with a targeted degree of polymerization of 87 (10000 g/mol). Figure 1b shows a plot of the normalized monomer concentration as a function of time as measured by in situ FTIR for an AGE polymerization utilizing **1**. The apparent propagation rate constant for **1** (k_{app}^1) was 4.8×10^{-3} s^{-1} ($[\mathbf{1}]_0$ = 97 mmol/L). Plots of monomer consumption over time for polymerizations utilizing compounds **2**–**4** are also present on the plot for comparison. Significantly, **1** represented a ca. 170-fold increase in polymerization rate over the first-reported MOB initiator, $[(Bn)_2NCH_2CH_2(\mu_2\text{-}O)Al(Et)_2{\cdot}Al(Et)_3$ (**2**). The increase in rate due to amine substitution alone represented an increase in k_{app} of 50-fold from the Bn_2N-functionalized MOB **4** to the Me_2N-functionalized MOB **1**. The conclusion from this rate increase is that the alkylamine affects the site of monomer coordination and enchainment at every propagation event, not just the first monomer addition associated with initiation as was proposed in previous work.[37,38]

Solution polymerizations using **1** were disproportionately slower in comparison with the rapid neat polymerizations. While a neat polymerization concluded after 16 min ($k_{app} = 4.8 \times 10^{-3}$ s^{-1}, $[\mathbf{1}]_0$ = 97 mM), solution polymerizations required 2 days for completion ($k_{app} = 1.6 \times 10^{-5}$ s^{-1}, $[\mathbf{1}]_0$ = 46 mM). In light of this apparent discrepancy, we attempted to determine the dependence of the polymerization rate on MOB **1** concentration. We monitored a series of AGE polymerizations at several MOB concentrations using ^{1}H NMR spectroscopy in d_6-benzene under isothermal conditions. The polymerization rates were calculated using the linear portion of the initial monomer consumption, which for these polymerizations utilized over 12 h of spectroscopic data, resulting in a change in monomer conversion of up to ca. 3%. The results are shown in Figure 2. Notably, the rate of polymerization increased exponentially with concentration of **1**. The heat released due to epoxide ring opening was first considered as a potential source for the unusually high dependence of rate on concentration of **1**. However, under our reaction conditions only negligible heating of the polymerization reaction would occur (<0.1 °C). We interpreted the experimentally measured rate (v in mM/min) as a function of $[\mathbf{1}]$ by fitting the rate (5) to $v = v_0(1 + e^{\kappa [1]})/2$, where κ describes the rate increase per unit concentration of $[\mathbf{1}]$ added to the system (κ in mM^{-1}), and v_0 is the rate of an uncatalyzed reaction (v_0 in mM/min). This empirical description is consistent with **1** possessing the characteristics of both initiator and catalyst, which would serve as a speculative explanation for the apparent autocatalytic polymerization.

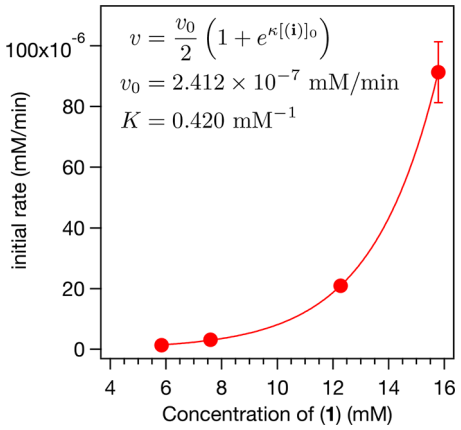

Figure 2. Initial polymerization rate measured under isothermal conditions by ^{1}H NMR spectroscopy in d_6-benzene at room temperature with no more than 3% conversion of AGE monomer. An apparent exponential dependence of polymerization rate on $[\mathbf{1}]$ was observed: $-d[AGE]/dt = v(t) = v_0(1 + e^{\kappa[\mathbf{1}]})/2$ with v_0 = (1.206 ± 0.003) × 10^{-7} mM/min as the polymerization rate in the absence of any catalytic activity and κ = 0.420 ± 0.002 mM^{-1} as the per unit concentration enhancement in rate due to catalytic activity.

Next, we explored the structural basis for the autocatalytic behavior of **1** giving rise to the unusual behavior in Figure 2.

Identification of the Polymerization Intermediate. To gain mechanistic insight, we attempted the synthesis of an analogue to the polymerization intermediate by the reaction of 2-(2-(dimethylamino)ethoxy)ethanol and triisobutylaluminum. We posit that this combination of reagents provided a model for the nascent propagating species after a single monomer enchainment of epoxide to the MOB, with the caveat that our model intermediate was formed via a route different from that for the true polymerization intermediate. The structure of the resultant complex **5** obtained by X-ray crystallography is shown in Figure 3. Detailed crystallographic data (Tables S7–S12) and NMR spectroscopy (Figures S2 and

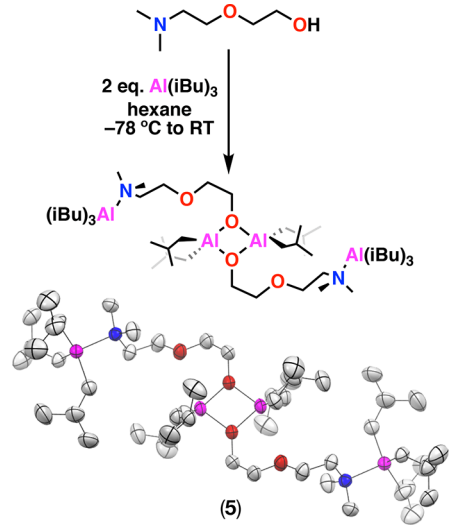

Figure 3. Proposed intermediate **5** synthesized from $Me_2NCH_2CH_2OCH_2CH_2OH$ and triisobutylaluminum according to the standard MOB synthetic procedure. The proposed intermediate is a dimer of MOBs with a dative N–Al bond between alkylamine and trialkylaluminum.

DOI: 10.1021/acscatal.8b02446
ACS Catal. 2018, 8, 8796–8803

S10) can be found in the Supporting Information. The symmetric structure of the resultant compound was unanticipated. In particular, **5** presented a bis((μ-alkoxo)-dialkylaluminum) (BOD) structure. Complex **5** was a dimeric complex of the monomeric MOB, as noted previously by Atwood et al. on related complexes.[40]

To substantiate if the purported intermediate **5** was representative of the polymerization intermediate, we first compared the rates of AGE polymerization using **1** and **5**. Similar polymerization rates produced by **1** and **5** would support that the BOD structure **5** may indeed be representative of the polymerization intermediate formed by MOBs **1**–**4**. All neat polymerizations were performed in duplicate at 60 °C. Aliquots of the active polymerization mixtures were taken at time points of 5, 10, 15, 20, 25, 30, 45, and 60 min, and conversion was determined by ^{1}H NMR spectroscopy of the remaining unreacted monomer in the crude reaction mixture. Under these conditions, **1** and **5** produced first-order consumptions of AGE monomer with $k_{app}{}^1$ of (1.40 ± 0.02) × 10^{-4} s^{-1} for **1** and $k_{app}{}^5$ = (1.62 ± 0.02) × 10^{-4} s^{-1} for **5**, as shown in Figure 4. The kinetic

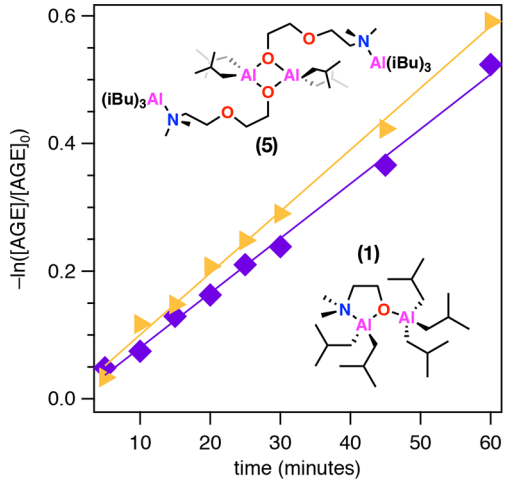

Figure 4. Comparison of polymerization rate using compounds **1** and **5**. Apparent rate constants were determined by fitting −ln[AGE]/[AGE]$_0$ = $k_{app}t$: $k_{app}{}^1$ = (1.40 ± 0.02) × 10^{-4} s^{-1}, $k_{app}{}^5$ = (1.60 ± 0.02) × 10^{-4} s^{-1} neat at 60 °C.

similarity between **1** and **5** under identical reaction conditions suggested that MOBs **1**–**4** may dimerize into BOD structures as the active polymerization intermediates (Scheme 2).

To obtain more direct evidence of a MOB to BOD transition, we utilized THF as a proxy monomer to observe MOB dimerization under conditions similar to those encountered in polymerization, but in the absence of chain growth. THF was titrated in increasing amounts to **1** in d_6-benzene, and ^{1}H NMR spectra were collected on the reaction mixtures. The ^{1}H NMR spectra are shown in Figure 5. As the THF concentration was increased, new peaks appeared and grew proportionally to the decrease in peaks associated with **1**. The positions of the new signals were similar to those observed from the proposed intermediate **5** in d_6-benzene (Figure S2). The reduced number of signals was consistent with the more symmetric, dimeric structure. The signals associated with the diatopic protons due to the bend in the N−C−C−O−AlR_3 plane of **1** converged into degenerate signals as THF was added, which was further consistent with symmetrization.

Scheme 2. Proposed MOB to BOD Transition to Active Polymerization Intermediate

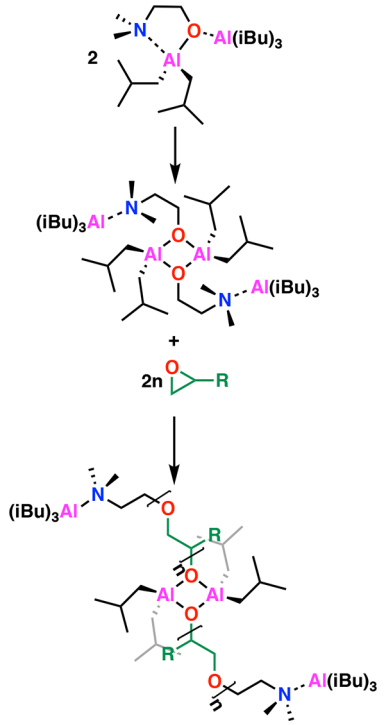

^{1}H−^{1}H correlated NMR spectroscopy (COSY) was also performed on the sample with 2 equiv of THF. Interpretation of the COSY spectrum suggested that there were two species present in solution; one set of peaks was attributed to the dimerized structure (Figure S3), and a separate set of signals was associated with the MOB. Likewise, in epoxide polymerization we propose that exposure of the MOB to epoxide monomer removes the datively bound AlR_3 and provokes MOB dimerization while the liberated alkylamine captures the mobile AlR_3 species. Details of the interpretations of the COSY spectrum can be found in Figure S3 in the Supporting Information. Combined, the NMR spectroscopy data provide further evidence that monomer induces the MOB → BOD dimerization, where the BOD serves as the active polymerization intermediate in MOB initiated epoxide polymerization. While these results provide evidence for the structure of the active polymerization species, they do not yet explain the steep increase in rate we see with changes in amine substitution and with increases in concentration of **1**.

Our previously proposed mechanism for MOB-initiated polymerization of epoxides was consistent with experimental kinetic observations on a homologous series of MOB initiators with variation in alkylaluminum substitution. The polymerization rate was proposed to be covariant with the bond length between the datively bound trialkylaluminum and aluminum alkoxide R_3Al-O,[37] which was proposed to be the site of monomer enchainment. The current 170-fold enhancement in polymerization rate with a change in alkylamine substitution is inconsistent with our earlier mechanistic interpretation that presented the alkylamine as passive in the polymerization mechanism. The new results suggest an alternative hypothesis: the aluminoxane ring may be acting as initiator and the site of monomer enchainment (see Figure S4 for electrospray ionization mass spectrometry showing end group structure of

DOI: 10.1021/acscatal.8b02446
ACS Catal. 2018, 8, 8796−8803

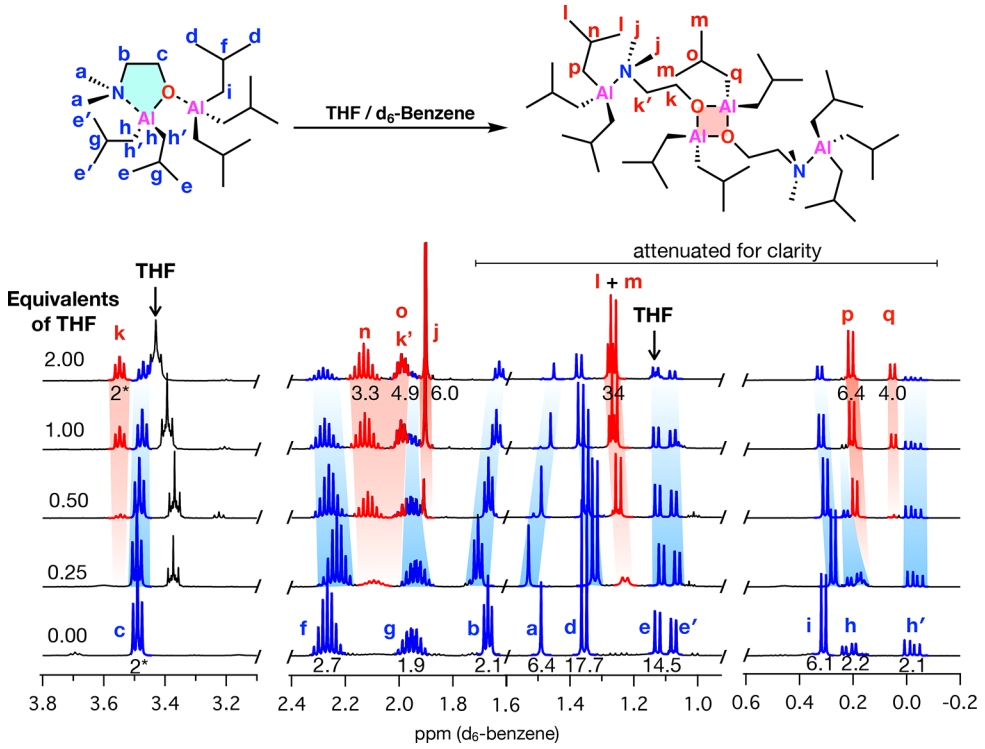

Figure 5. ^{1}H NMR spectra of **1** in d_6-benzene with increasing amounts of THF added. From bottom to top: 0.00, 0.25, 0.5, 1.0, and 2.0 equiv of THF. As the concentration of THF was increased, the peaks associated with the monomer species **1**, highlighted in blue, decrease and new peaks, highlighted in red, grow, which we attribute to the dimerized species. COSY spectra (Figures S3) further substantiate this interpretation. Integrals are indicated in black below the peaks. Asterisks indicate reference integrals.

a model poly(propylene oxide) synthesized for end-group determination), while the N−Al adduct, which forms upon MOB dimerization, may be acting as a catalyst as depicted in Figure 6. Merged initiation and catalytic functionalities would help explain the precipitous increase in polymerization rate with concentration of **1** shown in Figure 2. However, cooperativity is another possibility. To explore the possibility that the MOBs were acting as both catalyst and initiator, we decoupled the proposed initiation and catalytic moieties into discrete species.

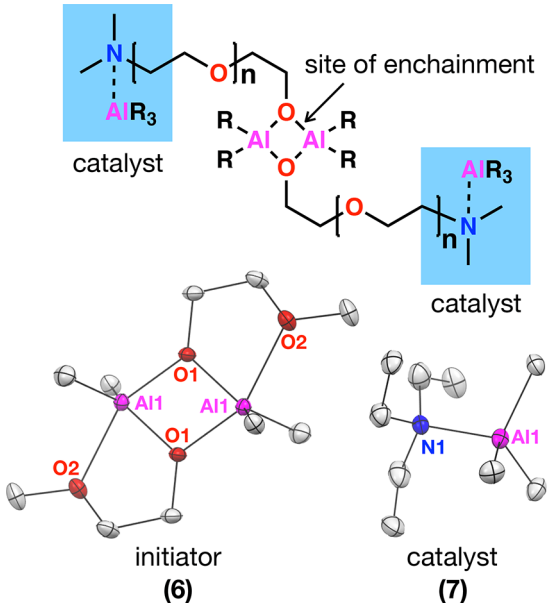

Figure 6. Distinct catalytic and initiation/propagation functionality of **1**−**5** separated into distinct initiator (**6**)[41] and catalyst (**7**) species.

Decoupling Catalytic and Chain-Growth Functionalities with Distinct N−Al Adduct Catalysts and Aluminum Alkoxide Initiators. An independent initiating BOD **6** and N−Al adduct **7** were synthesized to decouple the catalytic site from the site of chain growth. We synthesized the simple BOD structure **6** previously reported by Francis et al.[41] in a manner similar to that for **5** via the reaction of methoxyethanol and trimethylaluminum, which we hypothesize would provide a site for monomer addition and end-group control. The structure of **6** was verified by X-ray crystallography and can be seen in Figure 6, with further structural details given in Figure S11 and Tables S13−S18 in the Supporting Information. The adduct of triethylamine and trimethylaluminum (**7**) was synthesized by reacting the aforementioned compounds in hexane at −78 °C. These precursors were selected for synthetic convenience. The adduct was purified via crystallization. The structure of **7**, determined by X-ray crystallography, is shown in Figure 6. Detailed structural information can be found in Figure S12 and Tables S19−S24 in the Supporting Information. The formation of analogously stable alkylaluminum−alkylamine N−Al adducts has been reported previously.[42,43] Density functional theory calculations at the B3LYP/6-31++g(d,p) level of theory predict an N−Al bond dissociation energy of ca. −16 kcal/mol for **7**. Details of the calculation are given in Figure S13 in the Supporting Information. In order to determine how these species contribute to epoxide polymerizations, we incubated **6**, **7**, and **6** + **7** with AGE monomer and monitored the consumption of monomer over time. Figure 7 shows a plot of

DOI: 10.1021/acscatal.8b02446
ACS Catal. 2018, 8, 8796−8803

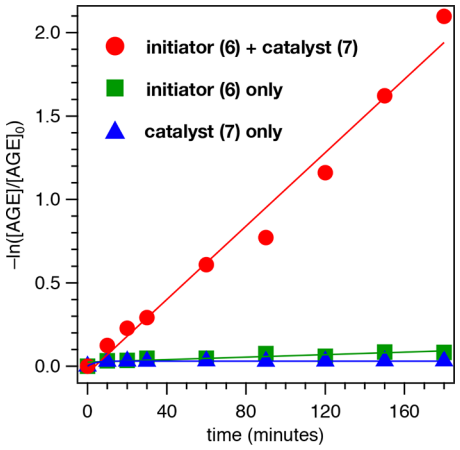

Figure 7. Plot of $-\ln[AGE]/[AGE]_0$ as a function of time for AGE polymerizations utilizING **6** (green squares), **7** (blue triangles), and combined **6** + **7** (red circles). The catalyst **7** alone did not produce polymer. Initiator **6** produced a slow polymerization. The polymerization rate increased precipitously when both initiator **6** and catalyst **7** were present.

$-\ln([AGE]/[AGE]_0)$ as a function of time. The slope of the line corresponds to k_{app} for the polymerization. From these data, the N−Al adduct catalyst **7** by itself does not polymerize AGE, while the BOD **6** initiator slowly polymerizes AGE, consistent with our previous work ($k_{app}^{6} = (9.48 \pm 1.21) \times 10^{-6}$ s^{-1}). Significantly, in the presence of both **6** and **7**, a significant increase in polymerization rate was observed. The enhanced rate was comparable to the performance of the structures **1** and (**5**) with $k_{app}^{6+7} = (1.78 \pm 0.06) \times 10^{-4}$ s^{-1}. This decisive result supports the assignment of catalytic activity to the N−Al adduct and the site of chain growth to the aluminum alkoxide. Electrospray ionization mass spectrometry of a model poly(propylene oxide) synthesized for determination of end-group structure is shown in Figure S5 and is consistent with a methoxyethanol end group derived from **6**. A key advantage of decoupling the chain-growth and catalytic functionalities is the potential for orthogonal control over molecular weight and polymerization rate. In a series of duplicate AGE polymerizations targeting 10000 g/mol, we increased the concentration of the N−Al adduct catalyst **7** to 1.0, 2.0, and 4.0 equiv relative to **6** and observed a significant increase in polymerization rate (Figure 8). The apparent rate constants increased significantly with N−Al concentration: 0.0 equiv of **7**, $k_{app}^{6} = (9.48 \pm 1.21) \times 10^{-6}$ s^{-1}; 1.0 equiv of **7**, $k_{app}^{6+7} = (1.78 \pm 0.06) \times 10^{-4}$ s^{-1}; 2.0 equiv of **7**, $k_{app}^{6+2\times7} = (17.2 \pm 0.12) \times 10^{-4}$ s^{-1}; 4.0 equiv of **7**, $k_{app}^{6+4\times7} = (69.0 \pm 10.5) \times 10^{-4}$ s^{-1}. Every added equivalent of **7** relative to initiator **6** produced an appreciable increase in k_{app} within the range of **7** concentrations explored. This result is reminiscent of the increase in polymerization rate seen with increasing concentration of **1** shown in Figure 2. The resultant molecular weights conformed closely to the targeted molecular weight of 10000 g/mol PAGE: 1.0 equiv of **7**, M_n = 9300 g/mol; 2.0 equiv of **7**, M_n = 8100 g/mol; 4.0 equiv of **7**, M_n = 7350 g/mol. The dispersities were respectively 1.34, 1.07, and 1.09. When we substituted the N−Al adduct **7** with trimethylaluminum, we observed a slower, nonliving polymerization (Figure S6) that terminated at low conversion (ca. 35%). We speculate that the dynamic and aggregating nature of alkylaluminum species led to a gradual transformation of $AlMe_3$ into a noncatalytic form

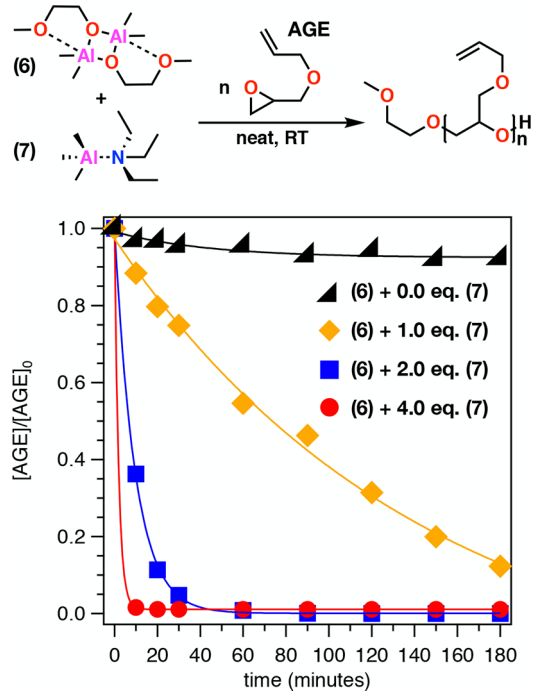

Figure 8. Unitless concentration of monomer $[AGE]/[AGE]_0$ versus polymerization time for initiator **6** (black triangle) and increasing amounts of N−Al adduct catalyst **7** relative to initiator **6**: 1.0 equiv of **7** (yellow diamonds); 2.0 equiv of **7** (blue squares); 4.0 equiv of **7** (red circles). All polymerizations were performed in duplicate.

during the polymerization. The persistence of the N−Al adduct (**7**) could be accounted for based on the increased stability of alkylaluminum species when coordinated by alkylamines.[42,44−49] ^{1}H−^{1}H COSY and NOESY experiments (Figures S7 and S8, respectively) were consistent with the persistence of the N−Al adduct in solution.

The polymerization kinetics of the N−Al adduct **7** in the presence of the initiator were consistent with the trends observed for the compounds with tethered catalyst and initiator **1**−**5**. All of the data exhibit a strong kinetic dependence on N−Al concentration, which suggests a consistent mechanism among **1**−**7**. We speculate that the high dependence of rate on catalyst concentration is due to cooperativity among N−Al species. Future work will focus on elucidating detailed structure−kinetics relationships for the N−Al adduct catalysts and the mechanistic basis for the high dependence of rate on catalyst concentration.

CONCLUSION

A new mono(μ-oxo)bis(alkylaluminum) (MOB) initiator was synthesized, which provided a considerable increase in the rate of polymerization for allyl glycidyl ether in comparison to previously reported homologous initiators for epoxide polymerization. New mechanistic insight was gained through isolation of a bis((μ-oxo)dialkylaluminum) (BOD) polymerization intermediate, which was corroborated by detailed NMR spectroscopy experiments. The change in structure of MOB precursor to BOD intermediate in the presence of datively coordinating moieties (e.g., epoxide, THF) and the strong dependence of polymerization rate on MOB/BOD concentration suggested the coupled catalytic and enchainment functionalities of the MOB/BOD system. This was verified by decoupling the associated moieties into distinct chemical

DOI: 10.1021/acscatal.8b02446
ACS Catal. 2018, 8, 8796−8803

species, which led to the isolation of a trialkylaluminum−trialkylamine (N−Al) adduct as a stable and effective catalyst for the living polymerization of epoxides. The N−Al adduct exhibited a strong dependence of polymerization rate on concentration similar to the MOB/BOD system, which suggested a consistent mechanism. The MOB initiators and N−Al adduct catalysts are unique and effective tools for the general polymerization of functional epoxides that offer control of molecular weight of structurally diverse polyethers in a short period of time under simple reaction conditions.

■ ASSOCIATED CONTENT

Supporting Information

The Supporting Information is available free of charge on the ACS Publications website at DOI: 10.1021/acscatal.8b02446.

Materials and methods anf additional spectra, chromatograms, mass spectrograms, computational details, and crystallographic data (PDF)

■ AUTHOR INFORMATION

Corresponding Author

*E-mail for N.A.L.: lynd@che.utexas.edu.

ORCID

Jennifer Imbrogno: 0000-0002-1526-5023
Robert C. Ferrier, Jr.: 0000-0002-5123-7433
Bill K. Wheatle: 0000-0003-0550-4905
Michael J. Rose: 0000-0002-6960-6639
Nathaniel A. Lynd: 0000-0003-3010-5068

Present Address

[‖]Department of Chemical Engineering and Materials Science, Michigan State University, East Lansing, MI, USA.

Notes

The authors declare no competing financial interest.

■ ACKNOWLEDGMENTS

The authors thank the Welch Foundation (F-1904) for support of this research. This research was partially supported by the National Science Foundation through the Center for Dynamics and Control of Materials: An NSF MRSEC under Cooperative Agreement No. DMR-1720595. The authors thank Dr. Vincent M. Lynch of the X-ray Diffraction Laboratory at the University of Texas at Austin in the Department of Chemistry. NMR spectra were collected on a Bruker Avance III 500 instrument funded by the NIH (1 S10 OD021508-01).

■ REFERENCES

(1) Obermeier, B.; Frey, H. Poly(ethylene glycol-co-allyl glycidyl ether)s: A PEG-Based Modular Synthetic Platform for Multiple Bioconjugation. *Bioconjugate Chem.* **2011**, *22*, 436−444.

(2) Obermeier, B.; Wurm, F.; Mangold, C.; Frey, H. Multifunctional Poly(ethylene glycol)s. *Angew. Chem., Int. Ed.* **2011**, *50*, 7988−7997.

(3) Wang, J.-S.; Matyjaszewski, K. Controlled/"Living" Radical Polymerization. Atom Transfer Radical Polymerization in the Presence of Transition-Metal Complexes. *J. Am. Chem. Soc.* **1995**, *117*, 5614−5615.

(4) Dias, E. L.; Nguyen, S. T.; Grubbs, R. H. Well-Defined Ruthenium Olefin Metathesis Catalysts: Mechanism and Activity. *J. Am. Chem. Soc.* **1997**, *119*, 3887−3897.

(5) Hillmyer, M. A.; Nguyen, S. T.; Grubbs, R. H. Utility of a Ruthenium Metathesis Catalyst for the Preparation of End-Functionalized Polybutadiene. *Macromolecules* **1997**, *30*, 718−721.

(6) Zhang, X.; Jones, G. O.; Hedrick, J. L.; Waymouth, R. M. Fast and Selective Ring-Opening Polymerizations by Alkoxides and Thioureas. *Nat. Chem.* **2016**, *8*, 1047−1053.

(7) Kiesewetter, M. K.; Shin, E. J.; Hedrick, J. L.; Waymouth, R. M. Organocatalysis: Opportunities and Challenges for Polymer Synthesis. *Macromolecules* **2010**, *43*, 2093−2107.

(8) Chuma, A.; Horn, H. W.; Swope, W. C.; Pratt, R. C.; Zhang, L.; Lohmeijer, B. G. G.; Wade, C. G.; Waymouth, R. M.; Hedrick, J. L.; Rice, J. E. The Reaction Mechanism for the Organocatalytic Ring-Opening Polymerization of L-Lactide Using a Guanidine-Based Catalyst: Hydrogen-Bonded or Covalently Bound? *J. Am. Chem. Soc.* **2008**, *130*, 6749−6754.

(9) Lohmeijer, B. G. G.; Pratt, R. C.; Leibfarth, F.; Logan, J. W.; Long, D. A.; Dove, A. P.; Nederberg, F.; Choi, J.; Wade, C.; Waymouth, R. M.; Hedrick, J. L. Guanidine and Amidine Organocatalysts for Ring-Opening Polymerization of Cyclic Esters. *Macromolecules* **2006**, *39*, 8574−8583.

(10) Yu, G.-E.; Heatley, F.; Booth, C.; Blease, T. G. Anionic Copolymerisation of Ethylene Oxide and Propylene Oxide. Investigation of Double-Bond Content by NMR Spectroscopy. *Eur. Polym. J.* **1995**, *31*, 589−593.

(11) Yu, G.-E.; Heatley, F.; Booth, C.; Blease, T. G. Anionic Polymerization of Propylene Oxide: Isomerization of Allyl Ether to Propenyl Ether End Groups. *J. Polym. Sci., Part A: Polym. Chem.* **1994**, *32*, 1131−1135.

(12) Hans, M.; Keul, H.; Moeller, M. Chain Transfer Reactions Limit the Molecular Weight of Polyglycidol Prepared via Alkali Metal Based Initiating Systems. *Polymer* **2009**, *50*, 1103−1108.

(13) Lee, B. F.; Wolffs, M.; Delaney, K. T.; Sprafke, J. K.; Leibfarth, F. A.; Hawker, C. J.; Lynd, N. A. Reactivity Ratios and Mechanistic Insight for Anionic Ring-Opening Copolymerization of Epoxides. *Macromolecules* **2012**, *45*, 3722−3731.

(14) Vandenberg, E. J. Organometallic Catalysts for Polymerizing Monosubstituted Epoxides. *J. Polym. Sci.* **1960**, *47*, 486−489.

(15) Morris, L. S.; Childers, M. I.; Coates, G. W. Bimetallic Chromium Catalysts with Chain Transfer Agents: a Route to Isotactic Poly(Propylene Oxide)S with Narrow Dispersities. *Angew. Chem., Int. Ed.* **2018**, *57*, 5731−5734.

(16) Huang, Y. J.; Qi, G. R.; Wang, Y. H. Controlled Ring-Opening Polymerization of Propylene Oxide Catalyzed by Double Metal-Cyanide Complex. *J. Polym. Sci., Part A: Polym. Chem.* **2002**, *40*, 1142−1150.

(17) Chruściel, A.; Hreczuch, W.; Janik, J.; Czaja, K.; Dziubek, K.; Flisak, Z.; Swinarew, A. Characterization of a Double Metal Cyanide (DMC)-Type Catalyst in the Polyoxypropylation Process: Effects of Catalyst Concentration. *Ind. Eng. Chem. Res.* **2014**, *53*, 6636−6646.

(18) Ghosh, S.; Lund, H.; Jiao, H.; Mejía, E. Rediscovering the Isospecific Ring-Opening Polymerization of Racemic Propylene Oxide with Dibutylmagnesium. *Macromolecules* **2017**, *50*, 1245−1250.

(19) Childers, M. I.; Vitek, A. K.; Morris, L. S.; Widger, P. C. B.; Ahmed, S. M.; Zimmerman, P. M.; Coates, G. W. Isospecific, Chain Shuttling Polymerization of Propylene Oxide Using a Bimetallic Chromium Catalyst: a New Route to Semicrystalline Polyols. *J. Am. Chem. Soc.* **2017**, *139*, 11048−11054.

(20) Ahmed, S. M.; Poater, A.; Childers, M. I.; Widger, P. C. B.; LaPointe, A. M.; Lobkovsky, E. B.; Coates, G. W.; Cavallo, L. Enantioselective Polymerization of Epoxides Using Biaryl-Linked Bimetallic Cobalt Catalysts: a Mechanistic Study. *J. Am. Chem. Soc.* **2013**, *135*, 18901−18911.

(21) Widger, P. C. B.; Ahmed, S. M.; Hirahata, W.; Thomas, R. M.; Lobkovsky, E. B.; Coates, G. W. Isospecific Polymerization of Racemic Epoxides: a Catalyst System for the Synthesis of Highly Isotactic Polyethers. *Chem. Commun.* **2010**, *46*, 2935−2937.

(22) Hirahata, W.; Thomas, R. M.; Lobkovsky, E. B.; Coates, G. W. Enantioselective Polymerization of Epoxides: a Highly Active and Selective Catalyst for the Preparation of Stereoregular Polyethers and Enantiopure Epoxides. *J. Am. Chem. Soc.* **2008**, *130*, 17658−17659.

(23) Peretti, K. L.; Ajiro, H.; Cohen, C. T.; Lobkovsky, E. B.; Coates, G. W. A Highly Active, Isospecific Cobalt Catalyst for

DOI: 10.1021/acscatal.8b02446
ACS Catal. 2018, 8, 8796−8803

Propylene Oxide Polymerization. *J. Am. Chem. Soc.* **2005**, *127*, 11566−11567.
(24) Tang, L.; Wasserman, E. P.; Neithamer, D. R.; Krystosek, R. D.; Cheng, Y.; Price, P. C.; He, Y.; Emge, T. J. Highly Active Catalysts for the Ring-Opening Polymerization of Ethylene Oxide and Propylene Oxide Based on Products of Alkylaluminum Compounds with Bulky Tetraphenol Ligands. *Macromolecules* **2008**, *41*, 7306−7315.
(25) Wasserman, E. P.; Annis, I.; Chopin, L. J.; Price, P. C.; Petersen, J. L.; Abboud, K. A. Ethylene Oxide Polymerization Catalyzed by Aluminum Complexes of Sulfur-Bridged Polyphenols. *Macromolecules* **2005**, *38*, 322−333.
(26) Rejsek, V.; Sauvanier, D.; Billouard, C.; Desbois, P.; Deffieux, A.; Carlotti, S. Controlled Anionic Homo- and Copolymerization of Ethylene Oxide and Propylene Oxide by Monomer Activation. *Macromolecules* **2007**, *40*, 6510−6514.
(27) Carlotti, S.; Billouard, C.; Gautriaud, E.; Desbois, P.; Deffieux, A. Activation Mechanisms of Trialkylaluminum in Alkali Metal Alkoxides or Tetraalkylammonium Salts/Propylene Oxide Controlled Anionic Polymerization. *Macromol. Symp.* **2005**, *226*, 61−68.
(28) Billouard, C.; Carlotti, S.; Desbois, P.; Deffieux, A. Controlled" High-Speed Anionic Polymerization of Propylene Oxide Initiated by Alkali Metal Alkoxide/Trialkylaluminum Systems. *Macromolecules* **2004**, *37*, 4038−4043.
(29) Akatsuka, M.; Aida, T.; Inoue, S. High-Speed "Immortal" Polymerization of Epoxides Initiated with Aluminum Porphyrin. Acceleration of Propagation and Chain-Transfer Reactions by a Lewis Acid. *Macromolecules* **1994**, *27*, 2820−2825.
(30) Aida, T.; Wada, K.; Inoue, S. Copolymerization of Epoxides by Aluminum Porphyrin - Reactivity of (Porphinato)Aluminum Alkoxide as Growing Species. *Macromolecules* **1987**, *20*, 237−241.
(31) Asano, S.; Aida, T.; Inoue, S. Immortal" Polymerization. Polymerization of Epoxide Catalysed by an Aluminium Porphyrin−Alcohol System. *J. Chem. Soc., Chem. Commun.* **1985**, 1148−1149.
(32) Aida, T.; Inoue, S. Living Polymerization of Epoxide Catalyzed by the Porphyrin-Chlorodiethylaluminum System. Structure of the Living End. *Macromolecules* **1981**, *14*, 1166−1169.
(33) Aida, T.; Inoue, S. Living Polymerization of Epoxides with Metalloporphyrin and Synthesis of Block Copolymers with Controlled Chain Lengths. *Macromolecules* **1981**, *14*, 1162−1166.
(34) Aida, T.; Mizuta, R.; Yoshida, Y.; Inoue, S. Polymerization of Epoxides Catalysed by Metalloporphine. *Makromol. Chem.* **1981**, *182*, 1073−1079.
(35) Gervais, M.; Labbé, A.; Carlotti, S.; Deffieux, A. Direct Synthesis of α-Azido, ω-Hydroxypolyethers by Monomer-Activated Anionic Polymerization. *Macromolecules* **2009**, *42*, 2395−2400.
(36) Roos, K.; Carlotti, S. Grignard-Based Anionic Ring-Opening Polymerization of Propylene Oxide Activated by Triisobutylaluminum. *Eur. Polym. J.* **2015**, *70*, 240−246.
(37) Ferrier, R. C.; Imbrogno, J.; Rodriguez, C. G.; Chwatko, M.; Meyer, P. W.; Lynd, N. A. Four-Fold Increase in Epoxide Polymerization Rate with Change of Alkyl-Substitution on Mono-μ-Oxo-Dialuminum Initiators. *Polym. Chem.* **2017**, *8*, 4503−4511.
(38) Rodriguez, C. G.; Ferrier, R. C., Jr; Helenic, A.; Lynd, N. A. Ring-Opening Polymerization of Epoxides: Facile Pathway to Functional Polyethers via a Versatile Organoaluminum Initiator. *Macromolecules* **2017**, *50*, 3121−3130.
(39) Dudev, T.; Lim, C. Ring Strain Energies From Ab Initio Calculations. *J. Am. Chem. Soc.* **1998**, *120*, 4450−4458.
(40) Atwood, D. A.; Gabbai, F. P.; Lu, J.; Remington, M. P.; Rutherford, D.; Sibi, M. P. Synthesis and Structural Characterization of Chiral Amine Alcohol Complexes of Aluminum. *Organometallics* **1996**, *15*, 2308−2313.
(41) Francis, J. A.; McMahon, C. N.; Bott, S. G.; Barron, A. R. Steric Effects in Aluminum Compounds Containing Monoanionic Potentially Bidentate Ligands: Toward a Quantitative Measure of Steric Bulk. *Organometallics* **1999**, *18*, 4399−4416.
(42) Bradley, D. C.; Coumbarides, G.; Harding, I. S.; Hawkes, G. E.; Maia, I. A.; Motevalli, M. Synthesis and Characterisation of Trialkylaluminium−Dialkylamine Adducts: X-Ray Diffraction and ^{1}H NMR Studies†. *J. Chem. Soc., Dalton Trans.* **1999**, 3553−3558.
(43) Davidson, N.; Brown, H. C. The Polymerization of Some Derivatives of Trimethylaluminum. *J. Am. Chem. Soc.* **1942**, *64*, 316−324.
(44) Lustig, C.; Mitzel, N. W. Molecularly Simple Dimethylaminomethyl Compounds of Aluminum, Gallium, and Indium. *Organometallics* **2003**, *22*, 242−249.
(45) Pfeiffer, M.; Murso, A.; Mahalakshmi, L.; Moigno, D.; Kiefer, W.; Stalke, D. Experimental and Computational Study on a Variety of Structural Motifs and Coordination Modes in Aluminium Complexes of Di(2-Pyridyl)Amides and -Phosphanides. *Eur. J. Inorg. Chem.* **2002**, *2002*, 3222−3234.
(46) Bessac, F.; Frenking, G. Chemical Bonding in Phosphane and Amine Complexes of Main Group Elements and Transition Metals †. *Inorg. Chem.* **2006**, *45*, 6956−6964.
(47) Ault, B. S. Matrix Isolation Study of the Reactions of Trimethylaluminum with Ammonia. *J. Phys. Chem.* **1992**, *96*, 7908−7912.
(48) Trinh, C.; Bodensteiner, M.; Virovets, A. V.; Peresypkina, E. V.; Scheer, M.; Matveev, S. M.; Timoshkin, A. Y. Chelating Ionic Versus Bridged Molecular Structures of Group 13 Metal Complexes with Bidentate Ligands. *Polyhedron* **2010**, *29*, 414−424.
(49) Biswas, K.; Chapron, A.; Cooper, T.; Fraser, P. K.; Novak, A.; Prieto, O.; Woodward, S. Dabbling with Air-Stable Organoaluminum Species. *Pure Appl. Chem.* **2006**, *78*, 511−518.

DOI: 10.1021/acscatal.8b02446
ACS Catal. 2018, 8, 8796−8803